Protective Efficacies of Formaldehyde-Inactivated Whole-Virus Vaccine and Antivirals in a Murine Model of Coxsackievirus A10 Infection

Zhenjie Zhang,[a] Zhaopeng Dong,[a,f] Juan Li,[a] Michael J. Carr,[b,c] Dongming Zhuang,[a] Jianxing Wang,[d] Yawei Zhang,[e] Shujun Ding,[d] Yigang Tong,[e] Dong Li,[f] Weifeng Shi[a]

Shandong Universities Key Laboratory of Etiology and Epidemiology of Emerging Infectious Diseases, Taishan Medical University, Taian, China[a]; Global Station for Zoonosis Control, Global Institution for Collaborative Research and Education (GI-CoRE), Hokkaido University, Sapporo, Japan[b]; National Virus Reference Laboratory, University College Dublin, Dublin, Ireland[c]; Department of Viral Infectious Diseases Control and Prevention, Shandong Center for Disease Control and Prevention, Jinan, China[d]; Beijing Institute of Microbiology and Epidemiology, Beijing, China[e]; School of Public Health, Taishan Medical University, Taian, China[f]

ABSTRACT Coxsackievirus A10 (CVA10) is one of the major pathogens associated with hand, foot, and mouth disease (HFMD). CVA10 infection can cause herpangina and viral pneumonia, which can be complicated by severe neurological sequelae. The morbidity and mortality of CVA10-associated HFMD have been increasing in recent years, particularly in the pan-Pacific region. There are limited studies, however, on the pathogenesis and immunology of CVA10-associated HFMD infections, and few antiviral drugs or vaccines have been reported. In the present study, a cell-adapted CVA10 strain was employed to inoculate intramuscularly 5-day-old ICR mice, which developed significant clinical signs, including reduced mobility, lower weight gain, and quadriplegia, with significant pathology in the brain, hind limb skeletal muscles, and lungs of infected mice in the moribund state. The severity of illness was associated with abnormally high expression of the proinflammatory cytokine interleukin 6 (IL-6). Antiviral assays demonstrated that ribavirin and gamma interferon administration could significantly inhibit CVA10 replication both *in vitro* and *in vivo*. In addition, formaldehyde-inactivated CVA10 whole-virus vaccines induced immune responses in adult mice, and maternal neutralizing antibodies could be transmitted to neonatal mice, providing protection against CVA10 clinical strains. Furthermore, high-titer antisera were effective against CVA10 and could relieve early clinical symptoms and improve the survival rates of CVA10-challenged neonatal mice. In summary, we present a novel murine model to study CVA10 pathology that will be extremely useful in developing effective antivirals and vaccines to diminish the burden of HFMD-associated disease.

IMPORTANCE Hand, foot, and mouth disease cases in infancy, arising from coxsackievirus A10 (CVA10) infections, are typically benign, resolving without any significant adverse events. Severe disease and fatalities, however, can occur in some children, necessitating the development of vaccines and antiviral therapies. The present study has established a newborn-mouse model of CVA10 that, importantly, recapitulates many aspects of human disease with respect to the neuropathology and skeletal muscle pathology. We found that high levels of the proinflammatory cytokine interleukin 6 correlated with disease severity and that ribavirin and gamma interferon could decrease viral titers *in vitro* and *in vivo*. Whole-virus vaccines produced immune responses in adult mice, and immunized mothers conferred protection on ne-

onates against challenge from CVA10 clinical strains. Passive immunization with high-titer antisera could also improve survival rates in newborn animals.

KEYWORDS HFMD, coxsackievirus A10, mouse model, antiviral, vaccine

Human enteroviruses (EVs) are positive-stranded RNA virus members of the genus *Enterovirus* within the family *Picornaviridae*, order *Picornavirales*, and comprise four species: EV-A, EV-B, EV-C, and EV-D (1). Coxsackievirus A10 (CVA10) belongs to species EV-A, which currently consists of 16 serotypes: 11 serotypes of coxsackievirus group A and 5 serotypes of EV (2, 3). In general, fatal cases of CVA10 infection have rarely been reported, as enterovirus A71 (EVA71) and CVA16 were the major epidemic strains prior to 2010 (4). However, numerous outbreaks of CVA10 have occurred during recent years in different geographic regions, such as China (5–8), Finland (9), and France (10). Clinical data demonstrated that CVA10 infections are commonly mild and self-limiting; however, a small proportion of children experience severe complications, such as, meningitis, encephalitis, acute flaccid paralysis, and neurorespiratory syndrome (11, 12). At present, due to the lack of effective antiviral drugs, CVA10 infection with severe complications is mainly treated with symptomatic and supportive therapy. Due to the recent increase in the incidence and severity of CVA10 infection, it is vitally important to understand the pathogenesis associated with this agent and to develop therapeutic drugs and vaccines (13).

In the present study, we established an animal model of CVA10 infection using 5-day-old neonatal mice in which the rapid proliferation of CVA10 was associated with clear pathology. Employing this model, we investigated the correlation between the expression of virus-induced inflammatory cytokines and disease severity and the antiviral effects of different drugs and therapeutic antibodies. Finally, we evaluated the immunoprotective effect of candidate CVA10 formaldehyde-inactivated whole-virus vaccines inoculated through different infection routes.

RESULTS

Establishment of a mouse model of CVA10 infection. Five-day-old neonatal mice were inoculated with CVA10 strain TA151R (Fig. 1) at different doses (1.0×10^2, 1.5×10^3, and 2.25×10^4 50% tissue culture infective doses [$TCID_{50}$] via the intramuscular [i.m.], intraperitoneal [i.p.], and intracerebral [i.c.] routes, respectively). Clinical signs, such as reduction in movement, appeared 5 to 6 days after low-dose inoculation (1.0×10^2 $TCID_{50}$), and the maximum clinical score was 3 (rounding to the nearest whole number) (Fig. 2A to C). At 9 to 10 days following low-dose inoculation (1.0×10^2 $TCID_{50}$), recovery and weight gain were observed (Fig. 2D to F), and the final survival rates were 70%, 80%, and 100% (Fig. 2G to I) for the mice inoculated via the i.m., i.p., and i.c. routes, respectively. These results suggest that the low infection dose (1.0×10^2 $TCID_{50}$) is unsuitable for 5-day-old neonatal Institute of Cancer Research (ICR) mice. Mice infected with 1.5×10^3 $TCID_{50}$ via the i.c. route did not show typical neurological symptoms (i.e., single or double hind limb paralysis), and only transient neonatal myasthenia gravis was observed. The average clinical score was 1.75 (Fig. 2C), and the survival rate was 60% (Fig. 2I). At the same dose, the mice inoculated via the i.m. and i.p. routes began to show clinical symptoms 3 days after inoculation, and the symptoms gradually worsened over time. The clinical score was 4 or 5 at 6 or 7 days after inoculation, with typical neurological symptoms (Fig. 2A and B). Compared with the control group, the body weight of the mice in the other two groups decreased by 28.71% and 19.19% (Fig. 2D and E). However, the clinical scores of the mice inoculated via the i.p. route had large variation and uneven distribution. The high dose (2.25×10^4 $TCID_{50}$) of CVA10 resulted in rapid disease onset in the neonatal mice and a short survival time (Fig. 2G to I), especially in the group inoculated via the i.m. route, where all the mice were dead 6 or 7 days after inoculation (Fig. 2G). This result indicated that the high dose (2.25×10^4 $TCID_{50}$) was also not suitable for the establishment of the CVA10 model. An intermediate dose (1.5×10^3 $TCID_{50}$) of CVA10 was administered to
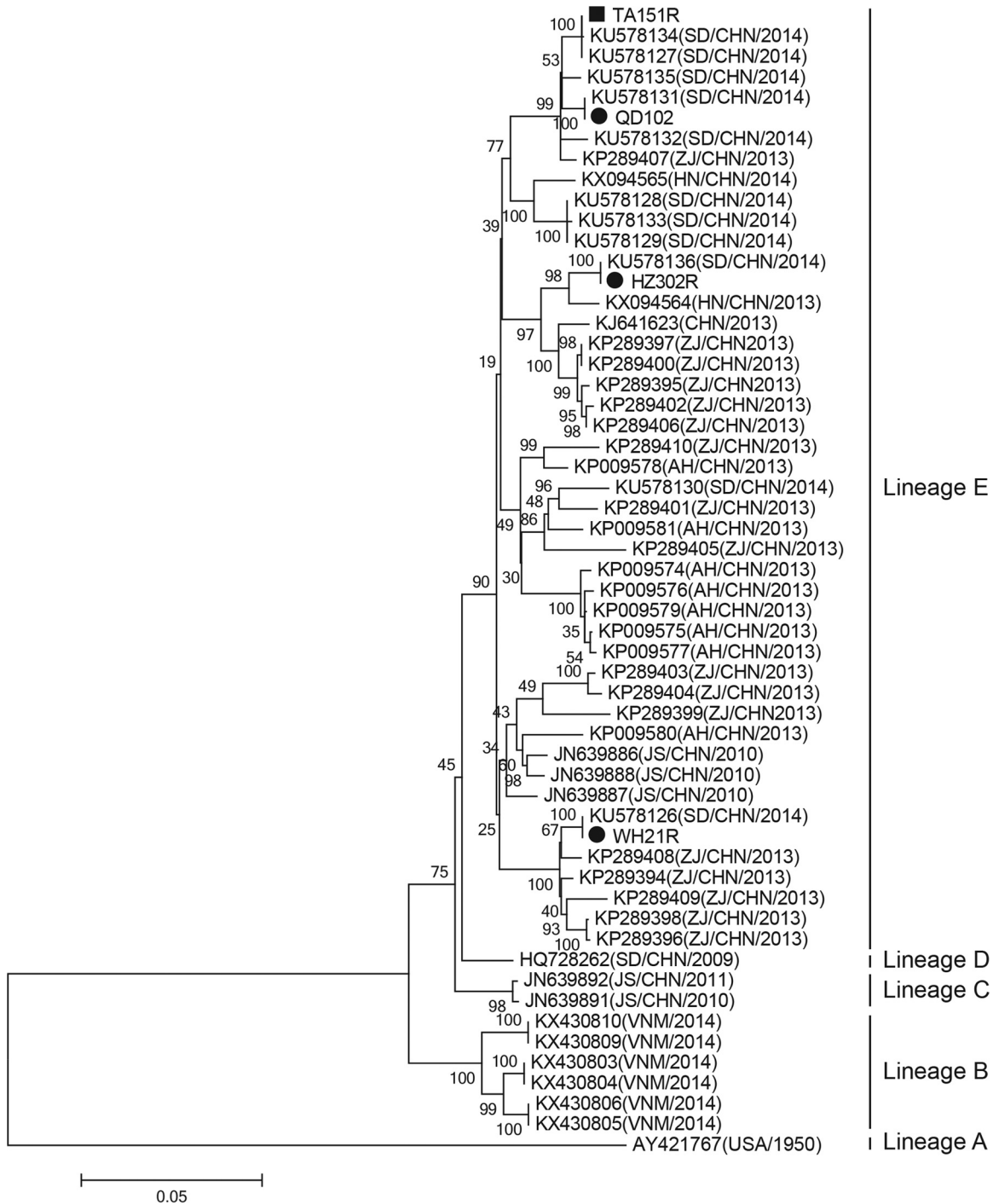
FIG 1 Phylogenetic tree based on the complete genome sequences of coxsackievirus A10 strains identified worldwide. Phylogenetic analysis of the four strains from Shandong Province and other strains ($n = 56$, including strains from China, Vietnam, and the United States) revealed that the four strains belonged to the same lineage (lineage E) and shared >98% homology with viruses circulating in China between 2010 and 2015. The maximum likelihood method was used to construct the phylogenetic tree, with 1,000 bootstrap replicates. Only strong bootstrap values (>70%) are shown. The scale bar represents the number of nucleotide substitutions per site. ■, TA151R strain used to establish the neonatal mouse model of CVA10 infection; ●, three clinical strains of CVA10 (WH21R, QD102R, and HZ302R) isolated from different regions of Shandong Province. CHN, China; VNM, Vietnam.

mice of different ages (3, 7, and 9 days) via the i.m. route, and the 3-day-old mice had high clinical scores and short survival times (Fig. 2J and K); the 7- and 9-day-old mice had low survival rates of 10% and 20% (Fig. 2L), respectively. Finally, the neonatal murine model of CVA10 infection was established by inoculating 5-day-old mice with
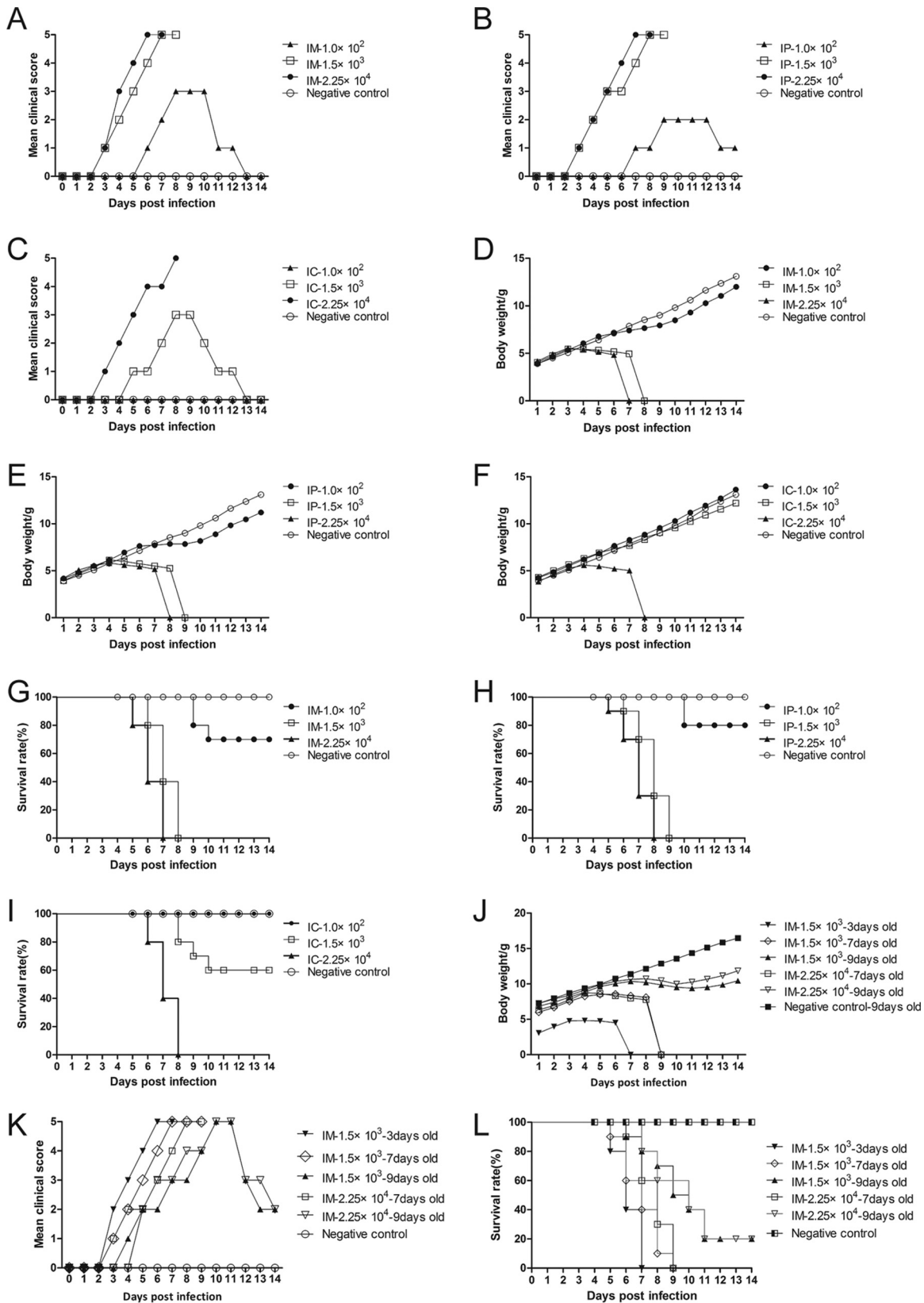
FIG 2 Determination of the optimal inoculation route, dosage, and age. Five-day-old ICR mice ($n = 10$ per group) were i.c., i.m., and i.p. inoculated with different doses of CVA10 strain TA151R (1.0×10^2, 1.5×10^3, and 2.25×10^4 $TCID_{50}$/mouse, respectively). Control animals were inoculated with medium. All the mice were monitored daily for clinical symptoms (A to C and K), body weight (D to F and J), and survival rates (G, H, and L) until 14 days postinfection. Mice at 14 and 21 days of age did not develop any significant clinical signs (data not shown). Control animals were administered NS. The data represent the mean values of the results of 10 repeat experiments.
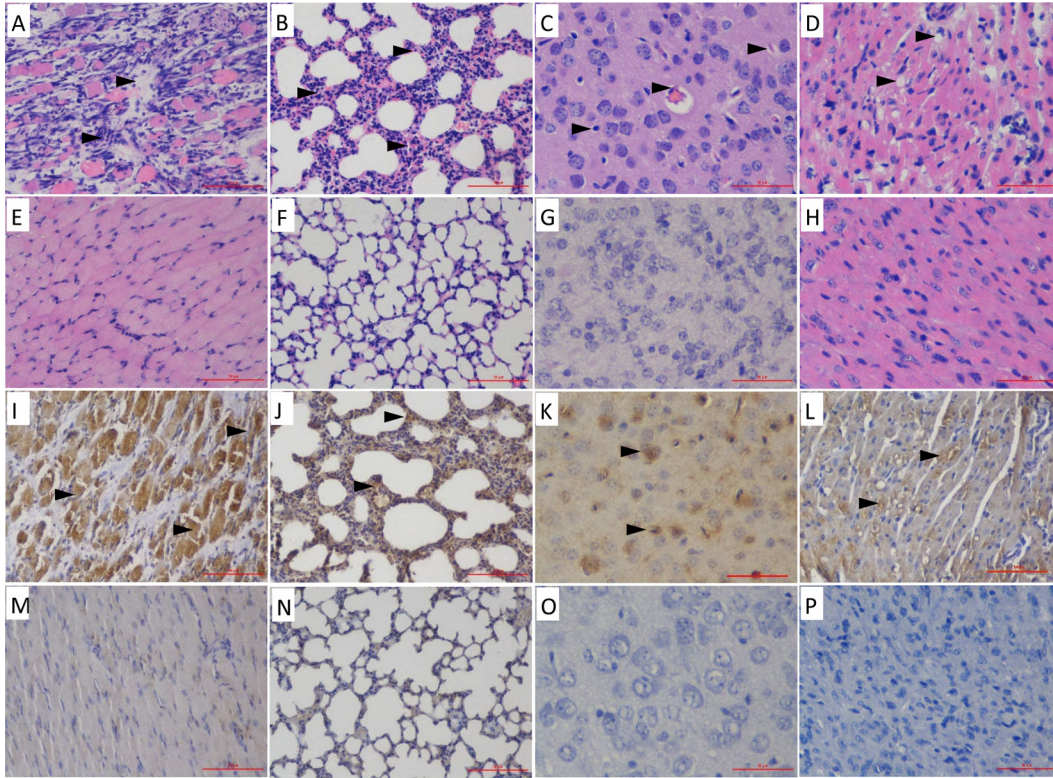
FIG 3 H&E and IHC analyses of infected 5-day-old mice after i.m. challenge with a lethal dose (240 LD_{50}) of CVA10 strain TA151R. (A to D) Infected mice (clinical grades, 4 and 5) exhibited severe necrosis in the contralateral hind limb muscle (A), lung (B), brain (C), and heart (D) tissue. (E to H) No histological changes were observed in the corresponding tissues of the mock-infected mice. (I to L) The IHC analysis indicated that the viral antigen was diffusely distributed in affected tissues: hind limb muscle (I), lung (J), brain (K), and heart (L). (M to P) Results for noninfected mice were used as a control: hind limb muscle (M), lung (N), brain (O), and heart (P). Magnification, ×400 (K and O); ×200 (others). All experiments were repeated three times.

1.5×10^3 $TCID_{50}$ of CVA10 via the i.m. route. The average clinical score was 4 to 5, and the mice died 8 to 9 days after inoculation. In this model, the disease onset time and mortality rates were stable and had good reproducibility.

Pathology and IHC. Hematoxylin and eosin (H&E) and immunohistochemistry (IHC) staining of the major tissues were performed 5 days after CVA10 inoculation in order to determine the pathological changes and antigenic distribution in tissues derived from the CVA10-infected neonatal mice. The results showed that the virus had strong tropism to the skeletal muscle and lung tissues (Fig. 3). Viral replication was associated with serious pathological damage, loose fiber, and massive necrosis, accompanied by large numbers of lymphatic infiltrates, muscle bundle fracture, and fibrosis (Fig. 3A). In addition, the lungs showed interstitial fibrosis and inflammatory hyperemia, which are typical clinical manifestations of severe interstitial pneumonia in neonates (Fig. 3B), with the virus diffusely distributed throughout the lung (Fig. 3J). In the brain tissue, the neurons and glial cells showed diffuse edema, and the nucleus was not completely lysed (Fig. 3C); the virus was mainly present in the cerebral cortex (Fig. 3K). Compared with EVA71 and CVA16 infections, CVA10 showed myocardial fiber dissolution and increased numbers of inflammatory cells, with focal fatty change (Fig. 3D) and detectable viral antigen (Fig. 3L). The other organs of the infected mice, such as liver, intestine, kidney, spleen, and lymph nodes, were also examined, but no significant histological changes or viral antigens were observed (data not shown).

CVA10 viral loads in organs of 5-day-old mice. After inoculation with TA151R (240 50% lethal doses [LD_{50}]) in 5-day-old mice, the virus loads at different time points and organs showed significant differences ($P < 0.05$) at 1, 3, 5, and 7 days postinfection (dpi). The viral loads indicated high viral replication in the early stages, and the viral
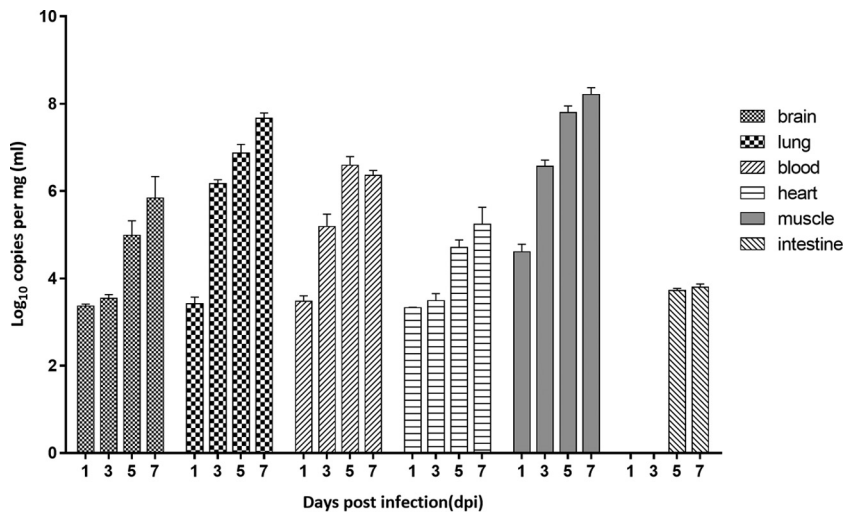
FIG 4 Mean tissue viral loads in CVA10-infected mice. Five-day-old ICR mice were i.m. inoculated with CVA10 strain TA151R (240 LD_{50}). The viral loads in brain, lung, heart, muscle, intestine, and blood from the infected mice were quantified by RT-qPCR. Samples were collected at the indicated times. The results represent the mean virus load (log_{10} copies) per milligram of tissue or per milliliter of blood and SD (three mice per group).

loads reached a maximum at 7 days after inoculation (Fig. 4). Viral loads were comparable in brain, lung, and heart tissues and in peripheral blood at 1 dpi and increased to 6 to 7 log_{10} copies/mg (ml) at 3 dpi. The onset time of viremia was correlated with clinical manifestations in the neonatal mice, including behavioral changes and decreases in body weight. At 7 dpi, the viral titers in lung tissues were as high as 7.7 log_{10} copies/mg, and the rapid viral proliferation was associated with severe pulmonary alveolar damage and large numbers of lymphocytic infiltrates, consistent with the pathological changes of viral pneumonia. In the early stage of infection, the viral load in skeletal muscles was an order of magnitude higher than that in other tissues, with significantly higher viral loads in the later stages than in other tissues, with the notable exception of brain tissue, which also had comparably higher viral loads at later time points (Fig. 4). In contrast, the virus was not detected in the intestines in the early stage of infection, and even during the late stages of infection, the viral load was <4 log_{10} copies/mg.

Expression of inflammatory cytokines in the peripheral blood of neonatal mice infected with CVA10 strain TA151R. After the 5-day-old ICR mice were infected with a lethal dose of TA151R, the expression of inflammatory cytokines in the peripheral blood was determined at different time points (Fig. 5). Compared with the negative-control (NC) group, inflammatory cytokines were highly expressed in the experimental group (Fig. 5). In particular, the expression of gamma interferon (IFN-γ) and interleukin 6 (IL-6) increased sharply (2,031 pg/ml and 2,028 pg/ml, respectively) and maintained a high level, although expression decreased slightly in the late stage of infection (Fig. 5A and B). The expression of IL-10 also increased initially, with a peak of 32.49 pg/ml, followed by a decrease from this maximum (Fig. 5C). The expression of IL-18 reached a peak of 212.80 pg/ml in the early stage (1 dpi) and maintained a high level of expression at all examined time points (Fig. 5D). The expression of IL-13 increased rapidly to 39 pg/ml in the early stages and then decreased to normal levels (less than the theoretical limit of detection of the assay, 1.17 pg/ml) at 4 dpi (Fig. 5E). In contrast, the expression of tumor necrosis factor alpha (TNF-α) did not show noticeable changes in the early stages of infection (Fig. 5F), and the expression level increased only in the later stage of infection. Finally, there was no detectable expression of IL-1β and IL-4 (data not shown). These results indicate that IL-6 and IFN-γ may be important factors in the immune response following CVA10 infection.
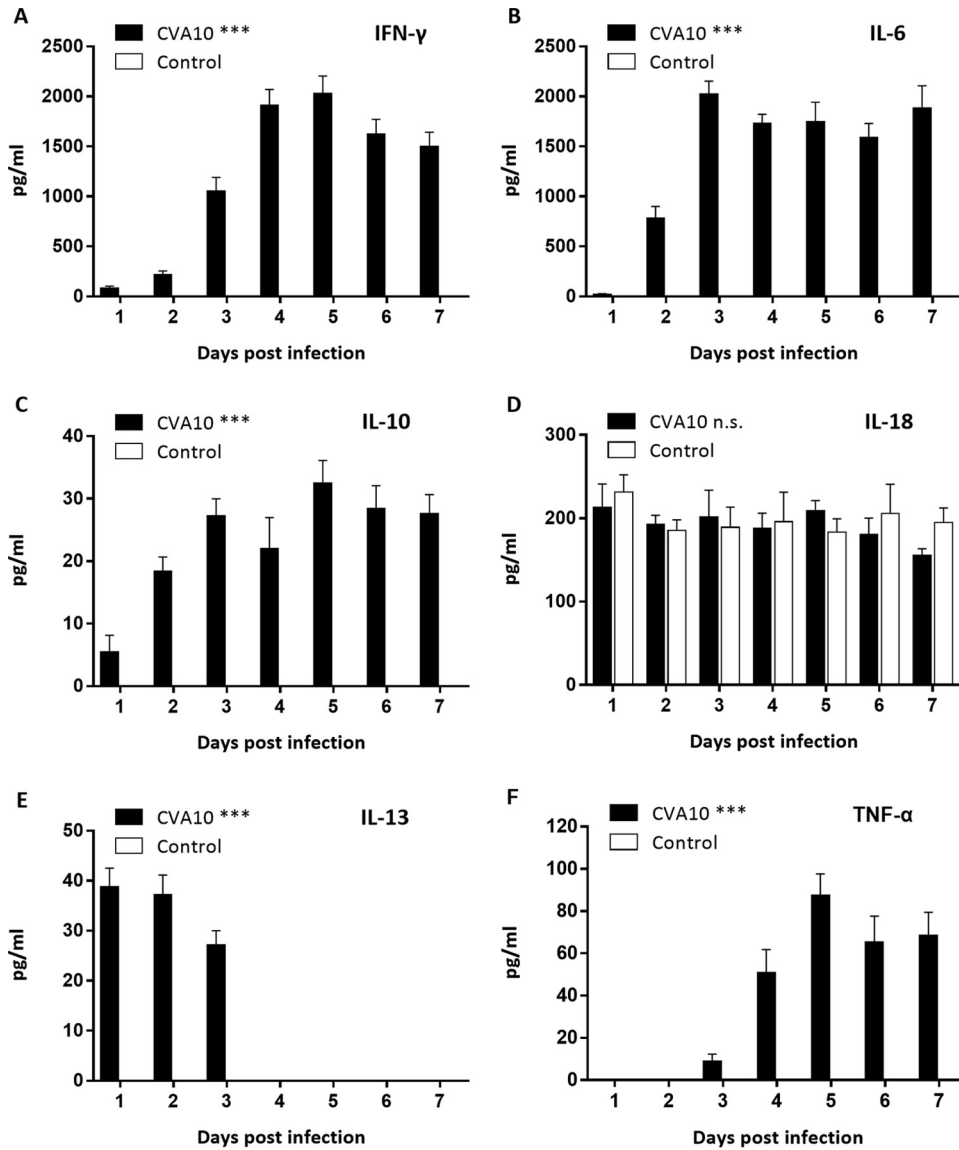
FIG 5 Peripheral cytokine/chemokine expression levels in neonatal mice infected with CVA10 with severe disease and in mock-infected controls were compared. The levels of IFN-γ (A), IL-6 (B), IL-10 (C), IL-18 (D), IL-13 (E), and TNF-α (F) in plasma of 5-day-old ICR mice i.m. inoculated with lethal doses of TA151R (240 LD_{50}) at 1 to 7 dpi were determined using mouse ELISA detection kits. IL-1β and IL-4 expression was not detected (data not shown). The data are shown as means and standard deviations and are representative of the results of at least 3 independent experiments. One-way analysis of variance (ANOVA) with a Newman-Keuls multiple-comparison test was used to compare the cytokine expression levels of neonates with severe disease and those of mock-infected animals. ***, $P < 0.001$; n.s., not significant.

In vitro and in vivo inhibition of CVA10 replication by cytokines and ribavirin. To assess the antiviral activities of drugs, antiviral assays were first performed on rhabdomyosarcoma (RD) cells. The RD cells were treated with IFNs and ribavirin 1 h after CVA10 infection. The growth of the RD cells was monitored by a cell counting kit 8 (CCK-8) assay, and the inhibitory rate on viral replication was calculated. Our results showed that the *in vitro* antiviral effects of ribavirin (20 μg), the type I interferons IFN-α1b (125 U) and IFN-α2a (125 U), and the type II interferon IFN-γ (25 U) were highest, with inhibitory rates of 31.73%, 24.7%, 23.89%, and 24.24% (Fig. 6A), respectively. In contrast, the *in vitro* antiviral effects of IFN-β (12.5 U), IFN-λ1 (125 ng), and IL-1β (1250 U) were weaker, with inhibitory rates of 13.62%, 3.69%, and 5.65%, respectively. There was no detectable antiviral effect of IL-6 (12.5 U) compared to the control group. Furthermore, the viral load of CVA10 in the supernatant of the ribavirin,
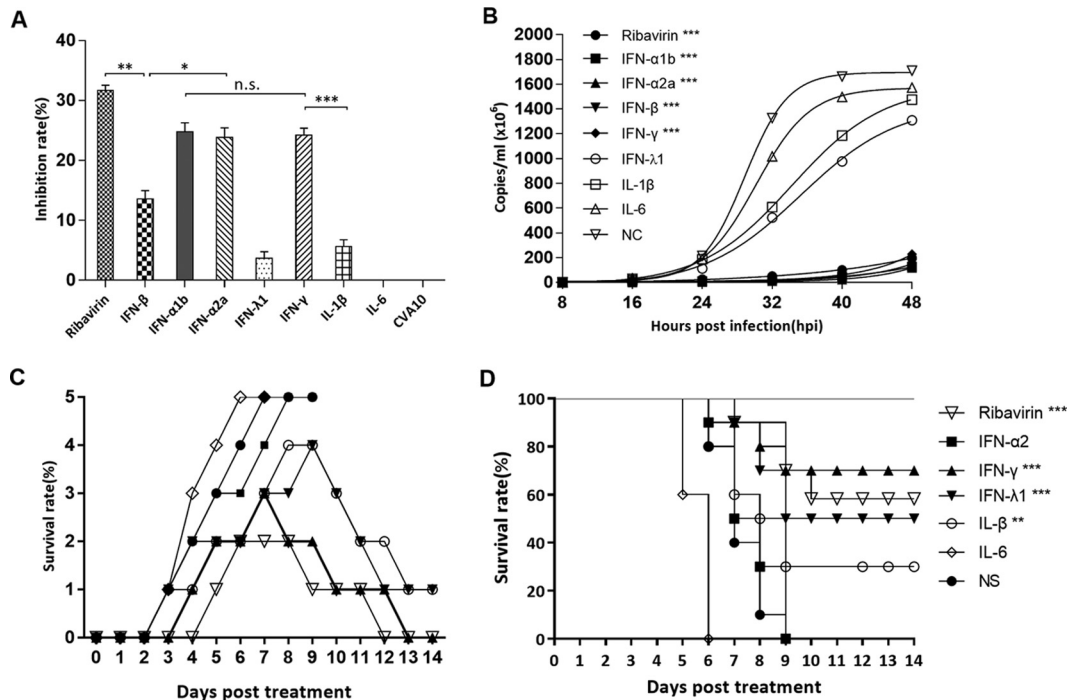
FIG 6 *In vitro* antiviral effects of ribavirin, IFN-α1b, IFN-α2a, IFN-β, IFN-γ, IFN-λ1, IL-1β, and IL-6 on CVA10. (A) RD cells were treated with different drugs for 4 h and then infected with CVA10 strain TA151R (MOI = 0.001). After culturing for 24 h, the viral inhibition rate was evaluated using a CCK-8 assay. (B) At 8-h intervals after RD cells were infected with TA151R, 100 μl of culture medium from each experimental and control group was taken out, and viral loads in the supernatant were determined by RT-qPCR. (C and D) Virus loads were expressed as $\log_{10}$ copies per milliliter, and statistical analysis was performed using one-way ANOVA with a Newman-Keuls multiple-comparison test. Clinical symptoms (C) and survival rates (D) were recorded daily after 5-day-old ICR mice (*n* = 10 per group) were i.m. challenged with lethal doses of TA151R (240 LD_{50}) until 12 dpi. Within 1 h postinoculation, each mouse was i.m. injected with the indicated cytokines. The data shown are expressed as means and SEM and are representative of at least 3 repeated experiments. The Mantel-Cox log rank test was used to compare the survival rates of pups between drug treatment groups and the medium control group. *, $P < 0.05$; **, $P < 0.01$; ***, $P < 0.001$; n.s., not significant.

IFN-α1b-, IFN-α2a-, IFN-β-, and IFN-γ-treated RD cells was lower ($<2 \times 10^8$ genome copies per ml) (Fig. 6B) than the viral load ($>1.2 \times 10^9$/ml) in the IFN-λ1-, IL-1β-, and IL-6-treated RD cells.

In vivo protection experiments were performed next, and after administration of a lethal dose of CVA10 (240 LD_{50}) via the i.m. route, therapeutic doses of ribavirin and IFNs were also injected by the intravenous (i.v.) route. The results showed that treatment of mice with different drugs had markedly different effects on survival rates (Fig. 6C and D). The survival rate of the mice in the ribavirin-treated (100 μg) group was 60%, and the survivors gradually recovered 8 days after treatment. All the mice treated with IFN-α2a (666.75 U) died (Fig. 6C), with no signs of recovery in the treated versus control groups. The protective rates of IFN-γ (833.25 U) and IFN-λ1 (1125 U) were 70% and 50%, respectively. In the IL-6-treated (1,000 U) group, the onset of symptoms occurred earlier than in the untreated group, with a shorter survival time (all the mice died by 6 dpi) (Fig. 6C), indicating that not only did IL-6 not have an antiviral effect, it increased the mortality rate.

Passive and active immunizations with the CVA10 antibody. The antibody titers of the CVA10 antiserum were measured by microneutralization assay. The titers of CVA10 (geometric mean titer [GMT], 2,048) were obtained by administering 2-fold serial dilutions of the CVA10 antiserum to RD cells. To evaluate the protective effect of the CVA10 antisera on the mice by passive immunization, 5-day-old mice were i.m. inoculated with 50 μl of 10-fold serially diluted antiserum (1:10 to 1:10,000), followed by inoculation with a lethal dose of TA151R (240 LD_{50}). Mice mock treated with normal saline (NS) began to show symptoms of hind limb paralysis at 5 dpi and died at 8 dpi.
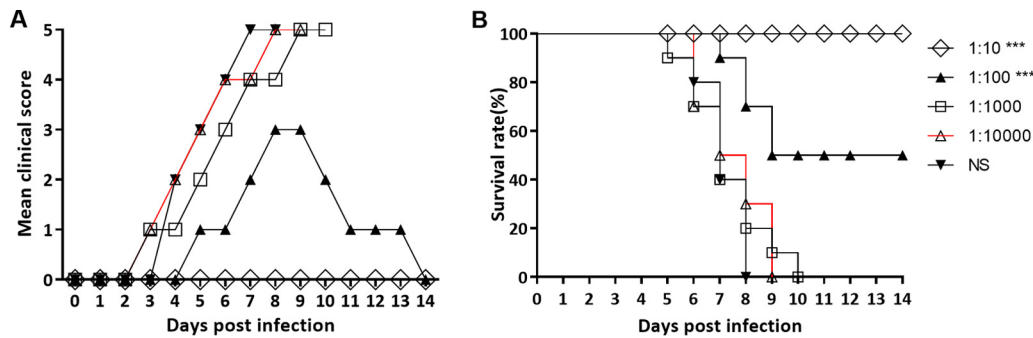
FIG 7 Passive immunization with anti-CVA10 serum protected neonates against CVA10 challenge *in vivo*. First, 5-day-old ICR mice (n = 10 per group) were i.m. inoculated with 240 LD_{50} of TA151R. Within 1 h after inoculation, each mouse was i.m. inoculated with 50 μl of 10-fold serially diluted mouse anti-CVA10 serum (10- to 10,000-fold dilutions) and negative serum. The clinical symptoms (A) and survival rates (B) were then monitored and recorded daily after inoculation with CVA10 until 14 days after inoculation. The Mantel-Cox log rank test was used to compare the survival of pups between the antiserum groups and the medium control group at 14 days postinfection. ***, $P < 0.001$.

In contrast, there were no clinical signs in the mice treated with the 10-fold-diluted CVA10 antiserum (Fig. 7A), and body weight was not significantly different from that of the control group, indicating the CVA10 antiserum could provide 100% immunoprotection to the infected mice (Fig. 7B). One hundredfold-diluted CVA10 antiserum could relieve the clinical signs, with a final protection rate of 50%. However, highly diluted (1:1,000 and 1:10,000) CVA10 antisera did not provide immunoprotective effects, and all the mice died at 9 to 10 dpi.

Furthermore, 8-week-old female mice were immunized twice with the candidate CVA10 inactivated vaccines and the control medium, respectively. After delivery, lethal doses of CVA10 clinical isolates were inoculated into the 5-day-old neonates by the i.m. route. There was no significant increase in body weight in the negative-control group. The clinical symptoms began to appear at 4 dpi, and all the mice died at 7 to 10 dpi (data not shown). In contrast, in the experimental group, the neonatal mice rapidly increased in body weight and did not show any clinical signs, with a final survival rate of 100%.

Evaluation of the therapeutic effects of CVA10 antiserum. To further evaluate the therapeutic effects of the CVA10 antiserum, neonatal mice with early- and late-onset disease, following a lethal dose of TA151R, were i.m. inoculated with different concentrations of the CVA10 antiserum. CVA10 antisera with higher dilution ratios afforded decreased levels of protection to the neonatal mice in the early stages of infection. The 10- and 100-fold-diluted CVA10 antisera deferred further development of the clinical syndromes in the neonatal mice (Fig. 8A), although some mice had transient hind limb paralysis. The clinical syndromes of >40% of the neonatal mice were improved (decreased clinical scores), and the final survival rates were 100% and 60% (Fig. 8B), respectively. However, there was no decrease of the clinical signs in the neonatal mice treated with the 1,000- and 10,000-fold diluted CVA10 antisera, and the mice died at 7 or 8 dpi, with no significant difference between the experimental group and the nonintervention group.

There was no therapeutic effect of the CVA10 antiserum in the neonatal mice with late-stage disease, with single hind limb or double hind limb paralysis in the dying mice (Fig. 8C and D). A range of dilutions of CVA10 antiserum (1:1, 1:10, and 1:100) could not prevent the progression of disease. There was also no significant difference in the progression of the clinical signs and the time of death in the neonatal mice between the experimental group and the positive-control group, and all the mice died 5 or 6 days after the antiserum intervention (Fig. 8C and D).

DISCUSSION

Establishment of a sensitive and reproducible animal model of CVA10 infection is critical for antiviral drug screening, vaccine development, and pathogenesis studies.
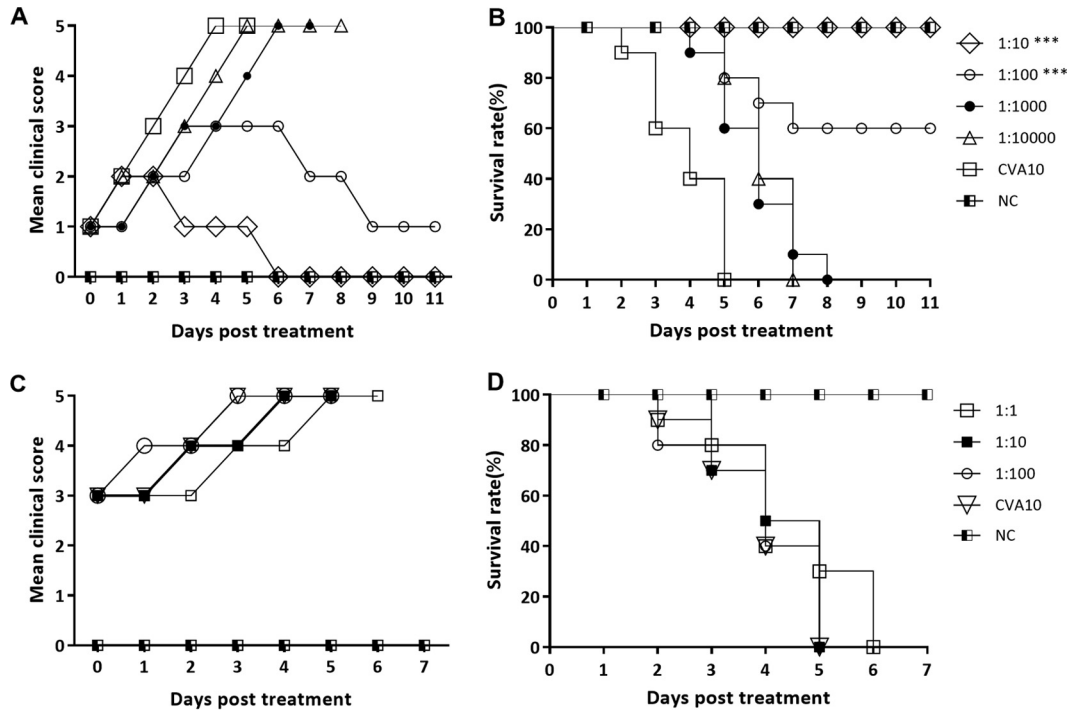
FIG 8 Therapeutic treatment with CVA10 antiserum reduces morbidity and mortality of neonatal mice against CVA10 challenge *in vivo*. Five-day-old ICR mice ($n = 10$ per group) were i.m. inoculated with 240 LD$_{50}$ of TA151R, which yielded a 100% mortality rate. Mice in early (grade, 1 or 2) and late (grade, >3) infection stages were selected ($n = 10$ per group) and intravenously injected with diluted CVA10 mouse antisera (1- to 10,000-fold dilutions, respectively). Clinical symptoms (A) and survival rates (B) of the mice in early stages of infection and clinical symptoms (C) and survival rates (D) of the mice in late stages of infection were recorded daily after inoculation with CVA10. The Mantel-Cox log rank test was used to compare the survival of pups between the antiserum groups and the medium control group. ***, $P < 0.001$.

The development of inactivated EVA71 vaccines is based on neonatal mouse and cynomolgus monkey models of viral infection (14–16). We have also shown that inactivated whole-virus vaccines were able to protect neonatal mice against coxsackievirus A6 infection (17). Therefore, inactivated vaccines have become the preferred choice for the prevention and control of CVA10-associated hand, foot, and mouth disease (HFMD) epidemics. A recent study reported that cell-adapted CVA10 strains could induce high titers of neutralizing antibody against homologous or heterologous CVA10 strains *in vitro* and *in vivo*, providing immunoprotection in infected neonatal mice (18). In the present study, we extend these findings by employing an animal model of CVA10 infection to investigate disease pathogenesis. After the 5-day-old neonatal mice were i.m. inoculated with CVA10 at a dose of 1.5×10^3 TCID$_{50}$, the virus was transmitted systematically from the inoculation site to several organs, including the central nervous system, lung, and skeletal muscle. Increased viral titers in blood and tissues were associated with the development of neurological symptoms, especially in hind limb muscles and lungs, and all the mice died 9 days after CVA10 infection. These results provide immunohistochemical and pathological evidence of CVA10 infection, which will be employed for further development of antivirals and vaccines and for pathological studies of CVA10-associated disease.

The expression of inflammatory cytokines was examined in order to identify factors that might be associated with the immunopathology seen in severe disease. Cerebrospinal fluid (CSF) IL-1β, IL-6, IL-8, and IFN-γ levels have been found to be significantly elevated in patients with pulmonary edema and encephalitis, with evidence of a strong correlation between proinflammatory cytokine production and clinical severity in EVA71 infections (19–21). Moreover, there were certain relationships between high levels of cytokine expression and increased blood vessel permeability (22). Similarly, our data showed that 3 days after inoculation with the CVA10 clinical strain TA151R,

5-day-old neonatal mice had increased expression of blood IL-6 and IFN-γ, showing a trend similar to that in the peripheral blood of children with HFMD (23). Abnormal expression of IL-6 may activate other immune cells and promote the release of inflammatory factors, leading to multiple-organ dysfunction syndrome through cascade pathways (24). In the present study, a high level of IL-6 in the peripheral blood of neonatal mice not only did not inhibit the replication of CVA10, but was associated with more severe clinical signs, with an average survival time 2 days shorter than that of the control group. Similar phenomena have also been observed in the CVA6 mouse model (17). In contrast, administration of anti-IL-6 neutralizing antibodies after the onset of clinical symptoms successfully improved the survival rates and reduced the clinical scores of the EVA71-infected mice (21). Collectively, these observations support the view that proinflammatory cytokines, especially IL-6 induced upon CVA6 infection, play prominent roles in the disease process. Although the high level of IFN-γ induced by CVA10 infection is involved in the innate immune clearance of the virus, it can also potentially lead to decreased IL-4 secretion in Th2 cells, resulting in an imbalance of the IFN-γ/IL-4 ratio, which is associated with severe immunopathology (25).

The nucleoside analogue ribavirin is a broad-spectrum antiviral drug and has been widely used for the treatment of viral hepatitis, lower respiratory tract infections, measles, and other viral infections (26, 27). We found that ribavirin significantly inhibited CVA10, with *in vitro* inhibition and *in vivo* protection rates of 32% and 60%, respectively. It has also been reported that interferon is effective against picornaviruses (EVA71 and theilovirus) and plays an important role in viral pathogenicity and tissue tropism (28, 29). Huang et al. attempted to treat EVA71-induced HFMD with IFN-α and found that IFN-α1b reduced the time to defervescence, healing times of typical skin or oral mucosal lesions, and EVA71 loads in children with HFMD (30). We found that IFN-α had no inhibitory effect on CVA10 replication *in vivo*, although the antiviral effect was significant *in vitro*. In contrast, the *in vivo* antiviral effect of IFN-λ1 was much greater than that observed *in vitro*, with an *in vivo* protective efficacy of 50% and a significantly shortened disease duration. Surprisingly, pretreatment with a clinically therapeutic dose of IFN-γ significantly increased the survival rate of the infected mice, up to 70%. The protective effect of IFN is highly correlated with the administration time (31). For example, when EVA71-infected mice were administered IFN at 3 dpi, the clinical symptoms of the neonatal mice were not relieved but deteriorated further. This may have been due to exacerbated IFN-γ-induced immune pathological damage (32).

The pathology associated with CVA10 infection progressed rapidly when severe complications and neurologic symptoms occurred. Our results showed that high antibody titer levels could relieve the clinical symptoms of neonatal mice in the early stages of infection and increase the survival rates of neonatal mice. However, administration of higher dilutions of CVA10 antibody could not prevent the development of the syndromes (grade, ≥3) in late-onset disease with single or double hind limb paralysis, and the course and severity of the disease were not significantly different from those of the control group; all the mice died at 10 dpi. In combination with the pathological changes and high viral loads in the tissues in the late stage of infection, severe inflammation and irreversible damage to various tissues and organs, such as nervous system destruction, neuronal necrosis, skeletal muscle fiber necrosis, and muscle bundle fracture, were found. Therefore, for neonatal mice with severe conditions, antibody therapy may be insufficient; symptomatic, supportive therapy and antiviral drug treatment should also be used.

It should be noted that 5-day-old mice are immunologically naïve, and the central nervous system is not yet mature. Although they have advantages in simulating severe cases of human infections with enteroviruses, it would be preferable to study pathogenesis in adult animals. In fact, we also performed infection experiments on older neonates (14 and 21 days); however, they did not show significant clinical symptoms, and all the challenged animals survived (data not shown). Therefore, adult transgenic mice that express the viral receptors (33) or adult AG129 mice deficient in type I and II

IFN receptors (34, 35), which are susceptible to enteroviruses, should be considered candidate animals in future studies.

In conclusion, we have established a sensitive and reproducible model of CVA10 infection. Using this model, we investigated the pathology of CVA10 infection and revealed a relationship between abnormal expression of IL-6-induced inflammatory cytokines and high mortality. Ribavirin and IFN-γ had the strongest *in vivo* and *in vitro* antiviral effects, and the survival rates of neonatal mice were significantly improved. Importantly, a formaldehyde-inactivated vaccine could induce immune responses, and also, maternal antibody could be transferred to neonatal mice. The maternal antibody provided cross-protection against challenge with lethal doses of CVA10 clinical isolates in the neonatal mouse model. Furthermore, when administered during early disease onset, CVA10 antiserum alleviated, and even reversed, disease in neonatal mice. Therefore, this mouse model of CVA10 infection provides a reliable tool for anti-CVA10 drug screening and vaccine development to develop therapies and prophylactic approaches to reduce the morbidity and mortality associated with HFMD.

MATERIALS AND METHODS

Ethics statement. The experimental animals were outbred, specific-pathogen-free ICR mice [certificate no. SCXK (Beijing) 2012-0001]. The feeding and processing of the animals were subject to the guidelines of the Technical Committee on Laboratory Animal Science of the Standardization Administration of China, and the study was carried out in accordance with the approved guidelines of the Ethics Committee of Taishan Medical College (permission no. 2016061).

Viruses and cells. RD cells (ATCC CCL-136) were cultured in minimum essential medium (MEM) (HyClone) containing 10% fetal bovine serum (FBS) (Gibco) at 37°C under 5% CO_2. CVA10 clinical strains (TA151R, WH21R, QD102R, and HZ302R) were isolated from fecal samples from 2- to 4-year-old patients who presented with HFMD in different cities of Shandong Province during 2015. The CVA10 viruses were serially passaged three times in RD cells, and the titers were determined by a $TCID_{50}$ assay. Total RNA was extracted, and the complete viral genomes were sequenced by standard methods.

Mouse infection experiments. To evaluate the pathogenicity of the TA151R strain in neonatal mice under different experimental conditions, an animal model of infection was established based on a two-factor analysis of variance, with the infective dose and the inoculation method as the two independent factors (three levels for each factor). For each inoculation dose and inoculation route experiment, 5-day-old neonatal mice were inoculated with different doses (1.0×10^2, 1.5×10^3, and 2.25×10^4 $TCID_{50}$/mouse) and also by different inoculation routes: i.c., i.m., and i.p., respectively. For age-dependent susceptibility assays, the susceptibility to CVA10 was compared for mice of different ages (3, 7, 9, 14, and 21 days), each inoculated by the i.m. route with a dose of 1.5×10^3 $TCID_{50}$. The body weight, clinical signs, and survival rates of the mice were monitored for 14 dpi. The grade of clinical disease was scored as reported previously (36), and scoring was carried out as follows: 0, healthy; 1, lethargy and inactivity; 2, hind limb weakness; 3, single limb paralysis; 4, double hind limb paralysis; and 5, death. The control mice were healthy throughout the experiments. The LD_{50} was calculated using the Reed and Muench formula (37).

Histopathologic and immunohistochemical staining. Five-day-old ICR mice were i.m. inoculated with the CVA10 clinical strain TA151R (240 LD_{50}) or uninfected culture medium. Tissue samples of brain, heart, lung, intestines, and contralateral hind limb skeletal muscles from control and CVA10-infected mice (grades, 4 to 5; $n = 3$) were dehydrated and embedded in paraffin according to procedures described previously (38). A microtome was used to generate 4-μm sections for histopathological examination, which were stained with hematoxylin and eosin.

Immunohistochemistry was performed using an avidin-biotin-immunoperoxidase technique as described previously (39). Briefly, tissue sections were dewaxed, dehydrated, and microwaved for 20 min at 99°C in a citrate buffer. Polyclonal mouse anti-CVA10 antibody (1:200 dilution; Abcam) was applied for 2 h at 37°C. A secondary biotinylated goat anti-mouse immunoglobulin G (1:1,000 dilution; Abcam) antibody was added, followed by avidin-biotin-peroxidase complex and 3,3'-diaminobenzidine tetrahydrochloride (Beyotime) chromogen. Tissues were counterstained with hematoxylin. The primary antibody was replaced by Tris-buffered saline or normal mouse serum in duplicate IHC assays and used as a negative control.

Virus loads in postchallenge mouse tissues. After inoculation of 5-day-old mice with lethal doses (240 LD_{50}) of TA151R via the i.m. route, tissues and blood samples (blood, brain, heart, lung, intestines, and contralateral hind limb skeletal muscles) from experimental mice ($n = 3$ per time point) were collected at 1, 3, 5, and 7 dpi and from control mice ($n = 3$) at the same time points. Total RNA was extracted from individual tissue/blood samples from infected mice and controls using TRIzol reagent (TaKaRa), and cDNA was generated by reverse transcription (RT) using random-hexamer primers and Moloney murine leukemia virus (MMLV) reverse transcriptase (TaKaRa), according to the manufacturer's instructions. The cDNA was then used for real-time PCR with a GoldStar TaqMan Mixture kit (CWBIO) and primers F-CA (5'-CCTGAATGCGGCTAATCC-3') and R-CA (5'-TTGTCACCATWAGCAGYCA-3') and a hydrolysis probe (5'-FAM [6-carboxyfluorescein]-CCGACTACTTTGGGWGTCCGTGT-BHQ1 [black hole quencher 1]-3') (40) in the ABI 7500 Fast System. Real-time PCR thermocycling reactions were as follows: 3 min at

95°C, followed by 40 cycles of 95°C for 15 s and 55°C for 35 s. The target amplicon amplified by the primers F-CV and R-CV was inserted into the pMD18-T plasmid, producing the plasmid pMD18-T-CV, which was used as a standard for absolute quantification of CVA10 copy numbers, with virus loads expressed as $\log_{10}$ copies/mg of tissue or $\log_{10}$ copies/ml of blood. The standard curve was generated from serially diluted pMD18-T-CV (ranging from 10^2 to 10^{10} copies/μl) by linear regression. The 95% confidence interval of the negative-control values determined in various organs and tissues was regarded as the reference value for methodological sensitivity (0 copies/mg or ml).

Cytokine assays. After inoculation of 5-day-old mice with lethal doses (240 LD_{50}) of TA151R via the i.m. route, peripheral blood was collected at 1, 2, 3, 4, 5, 6, and 7 dpi from the experimental and control groups and centrifuged for 10 min at $800 \times g$ at 4°C. Sera were frozen at -80°C until further examination. The levels of cytokines IL-1β, IL-6, IL-18, IFN-γ, and TNF-α; that of the anti-inflammatory cytokine IL-10; and those of the chemokines IL-4 and IL-13 were measured using mouse cytokine enzyme-linked immunosorbent assay (ELISA) kits (Multisciences Biotechnology) according to the manufacturer's instructions. The mean values of the replicates were used for statistical analysis.

***In vitro* and *in vivo* studies of antiviral inhibitory activities.** After the RD cells were inoculated with CVA10, the inhibitory effects of different drugs on CVA10 replication *in vitro* were measured using a CCK-8 kit (Multisciences Biotechnology), following the manufacturer's instructions. The RD cells were placed in 96-well plates (5×10^3 cells/well) and incubated overnight. When $>80\%$ confluent, the monolayers were infected with TA151R at a multiplicity of infection (MOI) of 0.001. After adsorption of CVA10 for 1 h, the supernatant was discarded and the RD cells were treated with the following concentrations of drugs: ribavirin, 20 μg; IFN-α2a, 125 U; IFN-β, 12.5 U; IFN-γ, 25 U; IFN-λ1, 125 ng; IL-1β, 1,250 U; and IL-6, 12.5 U. MEM was used as an NC. Four hours after treatment, the supernatant was discarded, and 500 μl of MEM containing 2% fetal bovine serum was added to each well. The cells were incubated at 37°C under 5% CO_2 for 36 h. The supernatant was discarded, and the cells were washed with phosphate-buffered saline (PBS) three times. After adding 200 μl of 10% CCK-8 solution, the cells were incubated for 1.5 h, and the absorbance of each cell was measured at 450 nm using a microplate reader (ELX-800; Biotek). The untreated RD cells were regarded as a reference, with 100% growth activity. The MEM-treated cells were used as a negative control. The ratio of growth activities was calculated by comparing the absorbances (optical density [OD]) of the cells in the control group and the reference group as follows: $SP\% = (A - A_1)/(A_2 - A_1) \times 100\%$, where SP represents the survival rate of the drug-treated RD cells and A, A_1, and A_2 are the OD values of cells in the experimental group, the reference group, and the negative-control group, respectively. After the RD cells were treated with TA151R for 48 h, the viral loads of the supernatants in the experimental and reference groups were determined by RT-quantitative PCR (qPCR) every 8 h. The mean values of the replicates were used for statistical analysis, and virus loads were expressed as $\log_{10}$ copies per milliliter.

In order to further examine the antiviral activities of the drugs in the neonatal mice, an *in vivo* antiviral assay was carried out. A lethal dose of TA151R (240 LD_{50}) was injected into the 5-day-old mice via the i.m. route. After 1 h of inoculation, different doses of the drugs were injected into the mice of the experimental group by the i.v. injection route, while NS was injected into the mice of the control group. The clinical signs and mortality were monitored and recorded daily until 14 dpi.

Preparation of formaldehyde-inactivated CVA10 strain TA151R whole-virus vaccines and determination of anti-CVA10 antibody titers. An inactivated CVA10 suspension with a formaldehyde concentration of 1:4,000 (vol/vol) was prepared by mixing 37% formaldehyde with CVA10 strain TA151R (1.1×10^7 $TCID_{50}$/ml). Ten milliliters of the suspension was mixed with Freund's adjuvant or Freund's complete adjuvant (Sigma) in equal volumes to produce an emulsion. The viral emulsion was then incubated at 37°C for 3 days (41). Ultrasonic emulsification was employed to prevent the formation of virus aggregates as follows: 2 ml of antigen-adjuvant mixture (1:1) was fully emulsified using sonication for 5 s at 5-s intervals a total of 8 times in an ice bath. No viable virus was detected after repeated RD cell culture and blind passage for up to 3 weeks. Eight-week-old adult ICR mice were inoculated with 50 μl of inactivated TA151R emulsion by the i.m. route. Blood of adult mice was collected 10 days after two immunizations with an interval of 2 weeks. The CVA10 antiserum was separated by centrifugation at $4,000 \times g$ for 10 min at 4°C and stored at -80°C until analysis.

The GMT of the neutralizing antibody in the CVA10 antiserum was determined by *in vitro* microneutralization assays as described previously (18) with slight modifications. Briefly, the anti-CVA10 serum samples were 10-fold serially diluted (1:10 to 1:10,000) using MEM containing 2% FBS. Fifty microliters of diluted serum was mixed with 100 $TCID_{50}$ of CVA10 strain TA151R in 96-well plates and incubated at 37°C for 1 h. Then, 5.0×10^3 RD cells were added to each well of the 96-well plate and cultured at 37°C under 5% CO_2. Three days later, the cells were inspected for cytopathic effect (CPE). Neutralization titers were determined as the highest serum dilution that could fully protect cells from CPE.

Effects of passive immunization and maternal antibody on 5-day-old neonatal mice. In order to study the protective effects of passive immunization, the CVA10 antiserum after 10-fold serial dilution (1:10 to 1:10,000) was injected into 5-day-old neonatal mice by i.v. injection ($n = 10$), while the same volume of NS was injected into the mice of the control group. After 24 h, a lethal dose of TA151R (240 LD_{50}) was inoculated into the mice in both groups by the i.m. route. The clinical signs and survival rates were monitored and recorded daily until 14 dpi.

To study the immunoprotective effects of maternal antibodies, neonatal mice were subcutaneously inoculated with 200 μl of Freund's complete adjuvant-inactivated CVA10 emulsion at 8 weeks of age, and the immune response was then boosted by inoculation with 200 μl Freund's adjuvant-inactivated CVA10 emulsion 2 weeks later. The female and male mice were mated after the first immunization, and the dams delivered 7 to 10 days after the second immunization. Mice in the control group were immunized with

the same volume of NS. A lethal dose (240 LD_{50}) of TA151R and the CVA10 clinical isolates WH21R (240 LD_{50}), QD102R (240 LD_{50}), and HZ302R (240 LD_{50}) (Fig. 1) were i.m. injected into the mice in the experimental group ($n = 10$) and the control group ($n = 10$). The clinical signs and survival rates were monitored and recorded for 14 dpi, and the immunoprotective effect of the maternal antibody on the neonates was evaluated.

Therapeutic effect of CVA10 antiserum on CVA10-challenged neonatal mice. In order to study the therapeutic effect of the CVA10 antiserum on the infected neonatal mice, a lethal dose of TA151R (240 LD_{50}) sufficient to induce 100% mortality was first administered to the 5-day-old neonatal mice by the i.m. route. The infected neonatal mice were quarantined. The neonatal mice with clinical scores of <3 and ≥3 were selected as the early and late treatment groups ($n = 10$ in each group), respectively. The CVA10 antiserum at different dilution ratios was administered by i.v. injection to the neonatal mice in the early and late treatment groups. The dilution ratios of the CVA10 antiserum were 1:10 to 1:10,000 and 1:1 to 1:100 for the early and late treatment groups, respectively. The body weight, clinical signs, and survival rates of the mice were monitored and recorded daily between 7 and 11 days posttreatment (dpt) to evaluate the therapeutic effect of the antiserum on the neonatal mice.

Statistical analysis. All statistical analysis was performed with GraphPad Prism version 5.0 (GraphPad 4 Software, San Diego, CA, USA). The frequencies of survival and mortality in treated mice versus control mice were assessed using Fisher's exact two-tailed test. The results were expressed as means and standard deviations (SD) of the means. Differences in the mean tissue viral titers, serum cytokine concentrations, and $TCID_{50}$s were determined using a two-tailed Mann-Whitney U test or Kruskal-Wallis test. The LD_{50} was calculated by the Reed and Muench method (37). A P value of <0.05 after two-tailed t testing was regarded as significant.

Accession number(s). The complete viral genome sequences have been submitted to GenBank (accession numbers KY272007 to KY272010).

REFERENCES

1. Knowles NJ, Hovi T, Hyypia T, King AMQ, Lindberg AM, Pallansch MA, Palmenberg AC, Simmonds P, Skern T, Stanway G, Yamashita T, Zell R. 2011. *Picornaviridae*, p 855–880. *In* 'King AMQ, Adams MJ, Carstens EB, Lefkowitz EJ (ed). 2012. Virus taxonomy. Classification and nomenclature of viruses. Ninth report of the International Committee on Taxonomy of Viruses. Elsevier Academic Press, London, United Kingdom.

2. Sun Q, Zhang Y, Zhu S, Tian H, Huang G, Cui H, Li X, Yan D, Zhu Z, Li J, Zheng P, Jiang H, Zhang B, Tan X, Zhu H, An H, Xu W. 2013. Transmission of human enterovirus 85 recombinants containing new unknown serotype HEV-B donor sequences in Xinjiang Uighur autonomous region, China. PLoS One 8:e55480. https://doi.org/10.1371/journal.pone.0055480.

3. Wang J, Zhang Y, Hong M, Li X, Zhu S, Yan D, Wang D, An H, Tsewang, Han J, Xu W. 2012. Isolation and characterization of a Chinese strain of human enterovirus 74 from a healthy child in the Tibet Autonomous Region of China. Arch Virol 157:1593–1598. https://doi.org/10.1007/s00705-012-1332-9.

4. Lu QB, Zhang XA, Wo Y, Xu HM, Li XJ, Wang XJ, Ding SJ, Chen XD, He C, Liu LJ, Li H, Yang H, Li TY, Liu W, Cao WC. 2012. Circulation of coxsackievirus A10 and A6 in hand-foot-mouth disease in China, 2009-2011. PLoS One 7:e52073. https://doi.org/10.1371/journal.pone.0052073.

5. Li W, Gao HH, Zhang Q, Liu YJ, Tao R, Cheng YP, Shu Q, Shang SQ. 2016. Large outbreak of herpangina in children caused by enterovirus in summer of 2015 in Hangzhou, China. Sci Rep 6:35388. https://doi.org/10.1038/srep35388.

6. Jiang FC, Yang F, Chen L, Jia J, Han YL, Hao B, Cao GW. 2016. Meteorological factors affect the hand, foot, and mouth disease epidemic in Qingdao, China, 2007-2014. Epidemiol Infect 144:2354–2362. https://doi.org/10.1017/S0950268816000601.

7. Yang Q, Ding J, Cao J, Huang Q, Hong C, Yang B. 2015. Epidemiological and etiological characteristics of hand, foot, and mouth disease in Wuhan, China from 2012 to 2013: outbreaks of coxsackieviruses A10. J Med Virol 87:954–960. https://doi.org/10.1002/jmv.24151.

8. He YQ, Chen L, Xu WB, Yang H, Wang HZ, Zong WP, Xian HX, Chen HL, Yao XJ, Hu ZL, Luo M, Zhang HL, Ma HW, Cheng JQ, Feng QJ, Zhao DJ. 2013. Emergence, circulation, and spatiotemporal phylogenetic analysis of coxsackievirus a6- and coxsackievirus a10-associated hand, foot, and mouth disease infections from 2008 to 2012 in Shenzhen, China. J Clin Microbiol 51:3560–3566. https://doi.org/10.1128/JCM.01231-13.

9. Blomqvist S, Klemola P, Kaijalainen S, Paananen A, Simonen ML, Vuorinen T, Roivainen M. 2010. Co-circulation of coxsackieviruses A6 and A10 in hand, foot and mouth disease outbreak in Finland. J Clin Virol 48:49–54. https://doi.org/10.1016/j.jcv.2010.02.002.

10. Mirand A, Henquell C, Archimbaud C, Ughetto S, Antona D, Bailly JL, Peigue-Lafeuille H. 2012. Outbreak of hand, foot and mouth disease/herpangina associated with coxsackievirus A6 and A10 infections in 2010, France: a large citywide, prospective observational study. Clin Microbiol Infect 18:E110–E118. https://doi.org/10.1111/j.1469-0691.2012.03789.x.

11. Fuschino ME, Lamson DM, Rush K, Carbone LS, Taff ML, Hua Z, Landi K, George KS. 2012. Detection of coxsackievirus A10 in multiple tissues of a fatal infant sepsis case. J Clin Virol 53:259–261. https://doi.org/10.1016/j.jcv.2011.12.011.

12. Yamashita T, Ito M, Taniguchi A, Sakae K. 2005. Prevalence of coxsackievirus A5, A6, and A10 in patients with herpangina in Aichi Prefecture. Jpn J Infect Dis 58:390–391.

13. Aswathyraj S, Arunkumar G, Alidjinou EK, Hober D. 2016. Hand, foot and mouth disease (HFMD): emerging epidemiology and the need for a vaccine strategy. Med Microbiol Immunol 205:397–407. https://doi.org/10.1007/s00430-016-0465-y.

14. Bek EJ, Hussain KM, Phuektes P, Kok CC, Gao Q, Cai F, Gao Z, McMinn PC. 2011. Formalin-inactivated vaccine provokes cross-protective immunity in a mouse model of human enterovirus 71 infection. Vaccine 29:4829–4838. https://doi.org/10.1016/j.vaccine.2011.04.070.

15. Ong KC, Devi S, Cardosa MJ, Wong KT. 2010. Formaldehyde-inactivated whole-virus vaccine protects a murine model of enterovirus 71 encephalomyelitis against disease. J Virol 84:661–665. https://doi.org/10.1128/JVI.00999-09.

16. Dong C, Wang J, Liu L, Zhao H, Shi H, Zhang Y, Jiang L, Li Q. 2010. Optimized development of a candidate strain of inactivated EV71 vaccine and analysis of its immunogenicity in rhesus monkeys. Hum Vaccin 6:1028–1037. https://doi.org/10.4161/hv.6.12.12982.

17. Zhang Z, Dong Z, Wei Q, Carr MJ, Li J, Ding S, Tong Y, Li D, Shi W. 2017. A neonatal murine model of coxsackievirus A6 infection for evaluation of

antiviral and vaccine efficacy. J Virol 91:e02450-16. https://doi.org/10.1128/JVI.02450-16.

18. Shen C, Liu Q, Zhou Y, Ku Z, Wang L, Lan K, Ye X, Huang Z. 2016. Inactivated coxsackievirus A10 experimental vaccines protect mice against lethal viral challenge. Vaccine 34:5005–5012. https://doi.org/10.1016/j.vaccine.2016.08.033.

19. Ye N, Gong X, Pang LL, Gao WJ, Zhang YT, Li XL, Liu N, Li DD, Jin Y, Duan ZJ. 2015. Cytokine responses and correlations thereof with clinical profiles in children with enterovirus 71 infections. BMC Infect Dis 15:225. https://doi.org/10.1186/s12879-015-0965-1.

20. Chen Z, Li R, Xie Z, Huang G, Yuan Q, Zeng J. 2014. IL-6, IL-10 and IL-13 are associated with pathogenesis in children with Enterovirus 71 infection. Int J Clin Exp Med 7:2718–2723.

21. Khong WX, Foo DG, Trasti SL, Tan EL, Alonso S. 2011. Sustained high levels of interleukin-6 contribute to the pathogenesis of enterovirus 71 in a neonate mouse model. J Virol 85:3067–3076. https://doi.org/10.1128/JVI.01779-10.

22. Weng KF, Chen LL, Huang PN, Shih SR. 2010. Neural pathogenesis of enterovirus 71 infection. Microbes Infect 12:505–510. https://doi.org/10.1016/j.micinf.2010.03.006.

23. Duan G, Yang H, Shi L, Sun W, Sui M, Zhang R, Wang X, Wang F, Zhang W, Xi Y, Fan Q. 2014. Serum inflammatory cytokine levels correlate with hand-foot-mouth disease severity: a nested serial case-control study. PLoS One 9:e112676. https://doi.org/10.1371/journal.pone.0112676.

24. Chung WH, Shih SR, Chang CF, Lin TY, Huang YC, Chang SC, Liu MT, Ko YS, Deng MC, Liau YL, Lin LH, Chen TH, Yang CH, Ho HC, Lin JW, Lu CW, Lu CF, Hung SI. 2013. Clinicopathologic analysis of coxsackievirus a6 new variant induced widespread mucocutaneous bullous reactions mimicking severe cutaneous adverse reactions. J Infect Dis 208:1968–1978. https://doi.org/10.1093/infdis/jit383.

25. Wang SM, Lei HY, Huang MC, Su LY, Lin HC, Yu CK, Wang JL, Liu CC. 2006. Modulation of cytokine production by intravenous immunoglobulin in patients with enterovirus 71-associated brainstem encephalitis. J Clin Virol 37:47–52. https://doi.org/10.1016/j.jcv.2006.05.009.

26. Riber CF, Hinton TM, Gajda P, Zuwala K, Tolstrup M, Stewart C, Zelikin AN. 2017. Macromolecular prodrugs of ribavirin: structure-function correlation as inhibitors of influenza infectivity. Mol Pharm 14:234–241. https://doi.org/10.1021/acs.molpharmaceut.6b00826.

27. Feld JJ, Hoofnagle JH. 2005. Mechanism of action of interferon and ribavirin in treatment of hepatitis C. Nature 436:967–972. https://doi.org/10.1038/nature04082.

28. Yi L, He Y, Chen Y, Kung HF, He ML. 2011. Potent inhibition of human enterovirus 71 replication by type I interferon subtypes. Antivir Ther 16:51–58. https://doi.org/10.3851/IMP1720.

29. Liu ML, Lee YP, Wang YF, Lei HY, Liu CC, Wang SM, Su IJ, Wang JR, Yeh TM, Chen SH, Yu CK. 2005. Type I interferons protect mice against enterovirus 71 infection. J Gen Virol 86:3263–3269. https://doi.org/10.1099/vir.0.81195-0.

30. Huang X, Zhang X, Wang F, Wei H, Ma H, Sui M, Lu J, Wang H, Dumler JS, Sheng G, Xu B. 2016. Clinical efficacy of therapy with recombinant human interferon α1b in hand, foot, and mouth disease with enterovirus 71 infection. PLoS One 11:e0148907. https://doi.org/10.1371/journal.pone.0148907.

31. McConnell J. 1999. Enteroviruses succumb to new drug. Lancet 354:1185.

32. Arya SC. 2000. Antiviral therapy for neurological manifestations of enterovirus 71 infection. Clin Infect Dis 30:988–992.

33. Koike S, Taya C, Kurata T, Abe S, Ise I, Yonekawa H, Nomoto A. 1991. Transgenic mice susceptible to poliovirus. Proc Natl Acad Sci U S A 88:951–955. https://doi.org/10.1073/pnas.88.3.951.

34. Khong WX, Yan B, Yeo H, Tan EL, Lee JJ, Ng JK, Chow VT, Alonso S. 2012. A non-mouse-adapted enterovirus 71 (EV71) strain exhibits neurotropism, causing neurological manifestations in a novel mouse model of EV71 infection. J Virol 86:2121–2131. https://doi.org/10.1128/JVI.06103-11.

35. Caine EA, Fuchs J, Das SC, Partidos CD, Osorio JE. 2015. Efficacy of a trivalent hand, foot, and mouth disease vaccine against enterovirus 71 and coxsackieviruses A16 and A6 in mice. Viruses 7:5919–5932. https://doi.org/10.3390/v7112916.

36. Liu Q, Shi J, Huang X, Liu F, Cai Y, Lan K, Huang Z. 2014. A murine model of coxsackievirus A16 infection for anti-viral evaluation. Antiviral Res 105:26–31. https://doi.org/10.1016/j.antiviral.2014.02.015.

37. Reed LJ, Muench H. 1938. A simple method of estimating 50 percent end-points. Am J Hyg 27:493–497.

38. Chang J, Li J, Liu X, Liu G, Yang J, Wei W, Zhang W, Yu XF. 2015. Broad protection with an inactivated vaccine against primary-isolated lethal enterovirus 71 infection in newborn mice. BMC Microbiol 15:139. https://doi.org/10.1186/s12866-015-0474-9.

39. Yu P, Gao Z, Zong Y, Bao L, Xu L, Deng W, Li F, Lv Q, Gao Z, Xu Y, Yao Y, Qin C. 2014. Histopathological features and distribution of EV71 antigens and SCARB2 in human fatal cases and a mouse model of enterovirus 71 infection. Virus Res 189:121–132. https://doi.org/10.1016/j.virusres.2014.05.006.

40. D'Ugo E, Marcheggiani S, Fioramonti I, Giuseppetti R, Spurio R, Helmi K, Guillebault D, Medlin LK, Simeonovski I, Boots B, Breitenbach U, Koker L, Albay M, Mancini L. 2016. Detection of human enteric viruses in freshwater from european countries. Food Environ Virol 8:206–214. https://doi.org/10.1007/s12560-016-9238-4.

41. Mao Q, Wang Y, Gao R, Shao J, Yao X, Lang S, Wang C, Mao P, Liang Z, Wang J. 2012. A neonatal mouse model of coxsackievirus A16 for vaccine evaluation. J Virol 86:11967–11976. https://doi.org/10.1128/JVI.00902-12.